THE ROLE OF N-LINKED GLYCOSYLATION IN DROSOPHILA DEVELOPMENT

by

Morgan Thomas

A thesis submitted to the Faculty of the University of Delaware in partial fulfillment of the requirements for the Honors Degree in Biological Sciences with Distinction

Spring 2016

THE ROLE OF N-LINKED GLYCOSYLATION IN DROSOPHILA DEVELOPMENT

by

Morgan Thomas

Approved: _____
Erica M. Selva, Ph.D.
Professor in charge of thesis on behalf of the Advisory Committee

Approved: _____
Jennifer Nauen, Ph.D.
Committee member from the Department of Biological Sciences

Approved: _____
Carlton Cooper, Ph.D.
Committee member from the Board of Senior Thesis Readers

Approved: _____
Michael Arnold, Ph.D.
Directory, University Honors Program

ACKNOWLEDGMENTS

It has been to my immense benefit that I have had a number of great individuals supporting me throughout my research career at Delaware. I'd like to thank Dr. Erica M. Selva for taking me under her wing as a sophomore, though I had few of the qualifications to work on such a complicated project, and teaching me how to think critically, problem solve independently, and develop the necessary skills to carry out an independent research project. She has been a great mentor throughout this process and has always made herself available to me, both as a mentor and a friend. I'd also like to thank Net, Brooke, and Matthew, past members of the Selva lab, who acted as a virtual encyclopedia of technical and scientific knowledge and who never tired of my endless questions. My labmates encouraged me through many failures and I am not sure I could have navigated through this sometimes difficult project without their help. This lab group has been like a second family to me and it will be truly missed. This project would not have been possible without the support and funding of the Undergraduate Research program and the Howard Hughes Medical Institute which supported my research through two Summer Scholars sessions. I would also like to thank HHMI for allowing me the opportunity to present my research nationally at the Experimental Biology meeting in 2016.

Lastly, I would like to thank my parents for encouraging me to follow my interests and get involved in research early in my college career. Research truly has taught me more than any other experience in college and I wouldn't have thought to put myself out there and find a lab if it hadn't been for your encouragement. Thank

you for supporting me through summers away from home and countless hours of complaining about how hard it is to dissect fruit fly eyes under a microscope. You guys are the best. I'd also like to thank Joshua, my constant companion through four years of labs and lectures. This journey wouldn't have been nearly as fun without you. This process has taught me so much about myself and my capabilities, and I am excited to apply the skills I have learned in the next chapter of my life as a student in the genetic counseling master's degree program at the University of Maryland School of Medicine.

TABLE OF CONTENTS

LIST OF TABLES vi
LIST OF FIGURES vii
ABSTRACT x

1 INTRODUCTION 1

1.1 The N-linked Glycosylation Pathway 1
1.2 *Asparagine-linked glycosylation 9* and *10* 2
1.3 Congenital disorders of glycosylation 3
1.4 The Unfolded Protein Response (UPR) 5
1.5 *Drosophila* as a Model 6
1.6 *Drosophila* eye development 8
1.7 Purpose and Specific Aims 10

2 METHODS 12

2.1 Stocks and stock maintenance 12
2.2 Virgin collection and genetic crosses 13
2.3 Generating genetic mosaics 13
2.4 Imaginal disc collection and dissection 15
2.5 Imaginal disc staining 17
2.6 Western blot analysis 18
2.7 Genetic rescue of *alg10* 19
2.8 XBP1-GFP assay 20

3 RESULTS 22

3.1 *alg9* and *alg10* eye discs show organizational irregularities 22
3.2 *alg9* and *alg10* eye discs show loss of axon adhesion and pathfinding 27
3.3 *alg9* and *alg10* eye discs show elevated levels of apoptosis 28

4 DISCUSSION 32

REFERENCES 37

A GENETIC CROSSES 40
B ANTIBODIES 41

LIST OF TABLES

Table 1.1 An identified CDG exists for almost every gene associated with the N-linked pathway. The genes and related disease relevant to this study are highlighted in yellow. The phenotypes of these diseases are pleotrophic and often difficult to diagnose (adapted from Jaeken 2014). 4

Table 2.1 Genotypes of all balanced stocks maintained for use in experiments. Virgin females and young males were used from each stock to create experimental crosses. 12

LIST OF FIGURES

Figure 1.1 Schematic illustration of the N-linked glycan assembly. The process is initiated on the cytoplasmic face of the ER (upper left) where it proceeds to the 7 sugar stage, which then flips into the ER lumen (lower left) where the process is completed. Enzymes involved in the biosynthesis that give rise to congenital disorders of glycosylation (CDG) when mutant are shown in red. Those that have not are blue. N-acetylglucosimine is represented by blue squares, mannose by green circles and glucose by blue circles. The red rectangles represent the dolichol phosphate linker (adapted from Hennet 2012). 2

Figure 1.2 The UPR pathway is mediated by three sensor proteins IRE1, PERK and ATF6. Each sensor protein stimulates an independent pathway in an attempt to correct ER stress. (Oslowski et al 2011).....6

Figure 1.3 The *Drosophila* lifecycle is divided into four separate phases: embryo, larval, pupal and adult. Flies of the third instar larval and the adult stages were used in this study (Hartwell, 2006). 7

Figure 1.4 A) The adult *Drosophila* eye is made up of over 750 lenses. B) Illustration of the ommatidial cluster including photoreceptors and support cells. C) Development of the ommatidia within the 3rd instar larval imaginal eye disc (anterior is up) D) Differentiation of photoreceptor cells within the ommatidia (Freeman 1997). 9

Figure 1.5 **:** Top: Rough eye phenotypes observed in adult eyes. Bottom: Light microscope images of toluidine blue stained plastic sections of adult eyes (adapted from McCague, 2013). 10

Figure 2.1 UAS-GAL4 is a transgenic tool native to yeast that allows special and temporal control of gene expression. In this study expression of FLP was controlled using this mechanism (Figure adapted from St. Johnson, 2002). 14

Figure 2.2 Gene expression was controlled using the *ey-Flp gmr-hid* system. Through site specific recombination, this results in eyes composed of homozygous mutant tissue in an otherwise heterozygous background. ..15

Figure 2.3 The third instar larva contains several imaginal discs that develop into adult features. The disc of interest in this study was the eye imaginal disc located behind the mouth hooks of the larva and attached to the lobes of the immature brain. Wing discs were dissected also for use as a control in some experiments (adapted from Cruz, 1993).....17

Figure 2.4 The IRE-1 dependent pathway of the UPR has two actions, the first is to splice XBP1 pre-mRNA into its translatable form. This action promotes cell survival. When prolonged stress occurs, IRE-1 activity switches to phosphorylate JNK, triggering a pro-apoptotic cascade (Tabas 2011). 20

Figure 2.5 XBP1-GFP expressing construct indicates successful induction of UPR. GFP expressing cells are experiencing intracellular stress and induction of UPR (Ryoo *et. al* 2007). 21

Figure 3.1 ELAV (green) is a pan-neuronal marker used to show the general organization of the ommatidia in the eye disc, green (top panels). Chaoptin (red, middle panels) is a cell surface axonal glycoprotein. The lower panels show the merged images. Images are organized anterior, right and posterior, left. *alg9* and *alg10* eye discs show retention of glycoprotein in the cell body. The lower panel shows merged images. In all images eye discs are oriented anterior right and posterior left. 23

Figure 3.2 Chaoptin (red) is a cell surface axonal glycoprotein that is normally localized in the axon. Both *alg9* and *alg10* mutants show retention of Chaoptin in the cell bodies. The *alg10* rescue shows localization of Chaoptin similar to the wild type control. ELAV is in green (top panels) and Chaoptin (red, middle panels). The lower panels show the merged images. 24

Figure 3.3 **:** Neuroglian, an integral membrane protein from the immunoblobulin super family, is retained in the cell bodies of *alg9* and *alg10* mutant eye discs. Normal localization patterns are to the membrane of both cell bodies and axons. ELAV is in green (top panels) and Neuroglian (red, middle panels). The lower panels show the merged images. 26

Figure 3.4 Axons leaving the eye disc via the optic stalk in the eye imaginal disc adopt a high level of organization (WT). This organization is disrupted in *alg9* and *alg10* mutant eyes. Neuroglian is shown in red. Neuroglian shows localization to both the axons and body of neural cells. In the mutant samples, axons exiting the eye disc through the optic nerve show decreased levels of organization. 28

Figure 3.6 Cleaved Caspase-3 is a marker of apoptosis. Both mutants show a significant increase in apoptosis compared to wild type. The *alg10* rescue shows reduced apoptosis. ELAV is in green (top panels) and cleaved caspase (red, middle panels). The lower panels show the merged images. In all images eye discs are orien ted anterior right and posterior left. 29

Figure 3.7 Caspase 3 staining indicates individual cells from each ommatidial cluster undergo apoptosis. All apoptotic events occur on the posterior edge of the eye disc where the oldest photoreceptors lie. ELAV is in green (top panels) and cleaved caspase (red, middle panels). The lower panels show the merged images. In all images eye discs are oriented anterior right and posterior left. 30

Figure 3.5 **:** Western blot of rhodopsin protein extracted from adult fly heads. *alg10* rescue shows expression levels significantly higher than *alg10* and comparable to wild type suggesting successful rescue of eye tissue. 31

ABSTRACT

Asparagine-linked or N-linked glycosylation is an important post-translational modification pathway that adds a 14-sugar oligosaccharide to target proteins on the luminal side of the endoplasmic reticulum. These glycan "tags" are necessary for multiple cellular functions including cell-cell recognition, protein trafficking, and proper protein folding. The focus of this study is to examine the effect of loss of function mutations in the N-linked pathway. A group of human diseases, congenital disorders of glycosylation (CDG), arise from mutations in the genes involved in various steps of this pathway. While CDGs display pleotropic phenotypes, most include neuronal defects. The two specific genes under study in this project are *alg9* and *alg10.* Each encode a glycosyltransferase that adds a sugar residue to the growing oligosaccharide chain. The *Drosophila* eye is used as a model organ to study the effects of these genes on neuronal development. In adult flies, these mutations yield a small rough eye phenotype, which is more severe in *alg9,* as it acts five steps before *alg10* in the pathway. In order to determine the basis of this phenotype, larval eye discs were dissected, stained for different glycoprotein and neuronal markers, and then imaged using confocal microscopy. We found these mutations interrupt proper glycoprotein trafficking, as the axonal surface glycoprotein Chaoptin accumulates in the cell bodies of *alg9* and *alg10* mutant photoreceptors. Caspase-3 staining showed this accumulation eventually leads to photoreceptor apoptosis. Photoreceptor death likely continues through pupal development resulting in a reduced number of photoreceptors in *alg10* adult eyes and almost complete absence in *alg9* adult eyes.

These results indicate that CDG patients may have normal neuronal specification and differentiation, but experience neuronal deficits due to intracellular accumulation of glycoproteins leading to cell death. These data suggest markers of endoplasmic reticulum stress and the unfolded protein response should be examined in the future.

Chapter 1

INTRODUCTION

1.1 The N-linked Glycosylation Pathway

The N-linked glycosylation pathway is a post-translational modification pathway that effects proteins in the secretory system. Because of its universally important nature, the pathway is highly conserved from *Drosophila* to humans. Glycoproteins play important roles in many cellular processes including cell-cell adhesion and regulation of signaling molecules in the extracellular matrix.

During this process a 14-sugar oligosaccharide is generated in a stepwise fashion by enzymes in proximity to the endoplasmic reticulum (ER) membrane, first on the cytoplasmic side and later in the ER lumen. These enzymes catalyze the transfer of single sugar residues: two N-acetylglucosamine, nine mannose, and three glucose, to the growing chain attached to a dolichol phosphate linker embedded in the ER membrane. The finished 14 sugar glycan is then transferred en masse to a selected asparagine residue on a target protein in the lumen. These glycoproteins then undergo further modifications in the cytosol before reaching their final destinations (Burda & Aebi). The schematic below (Figure 1.1) shows the stepwise manner in which the oligosaccharide is built in the ER.

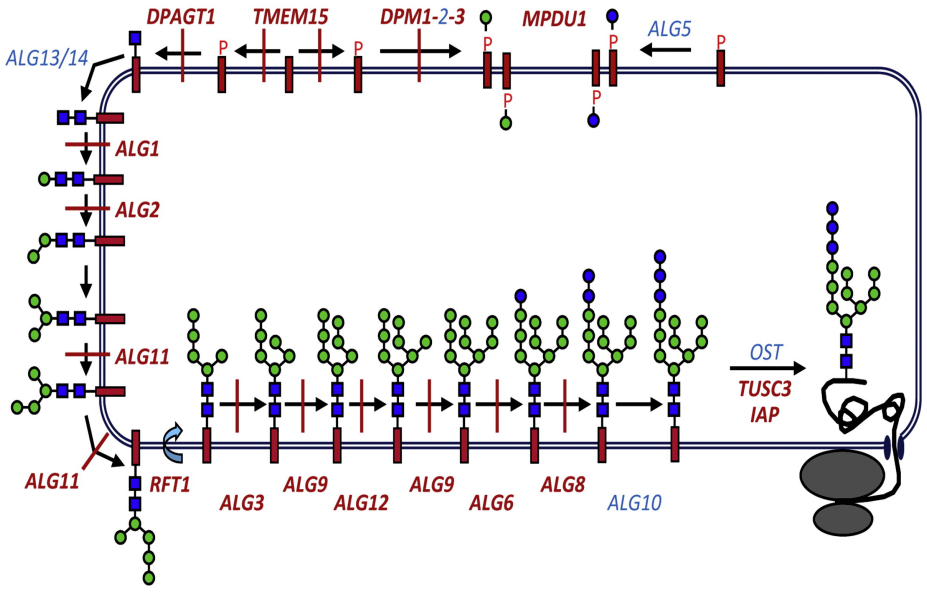

Figure 1.1 Schematic illustration of the N-linked glycan assembly. The process is initiated on the cytoplasmic face of the ER (upper left) where it proceeds to the 7 sugar stage, which then flips into the ER lumen (lower left) where the process is completed. Enzymes involved in the biosynthesis that give rise to congenital disorders of glycosylation (CDG) when mutant are shown in red. Those that have not are blue. N-acetylglucosimine is represented by blue squares, mannose by green circles and glucose by blue circles. The red rectangles represent the dolichol phosphate linker (adapted from Hennet 2012).

1.2 *Asparagine-linked glycosylation 9* and *10*

The two subject genes of our study, *alg9* and *alg10*, encode multipass integral membrane sugar transferases involved in the post-translational protein modification pathway known as the N-linked glycosylation pathway. *alg10* is a glycosyltransferase that catalyzes the addition of the terminal glucose reside to the dolichol-linked oligosaccharide in the endoplasmic reticulum (ER) prior to transfer of the oligosaccharide to nascent polypeptides during N-glycosylation. This glucose addition results in a complete core oligosaccharide. *alg9* encodes an α-1,2-mannosyltransferase, which acts twice in the pathway. It first catalyzes the addition of

a mannose residue to the α-1,3-linked mannose and then to the α-1,6-linked mannose. Each of these steps acts prior to *alg10* in the N-linked pathway (Figure 1.1). *alg9's* role in embryonic development is not yet known. The Selva lab has found in previous studies that mutations in these proteins cause defects in the embryonic central nervous system (CNS) (McCague 2013). We have already shown that *alg9* and *alg10* are required for proper embryo development, and that a mutation of *alg9* produces a more severe phenotype than *alg10***.**

It is hypothesized that this is due to the nature of the oligosaccharide transferase (Ost) responsible for catalyzing the addition of the complete oligosaccharide to its target protein. Ost has two isoforms, which are both found in *Drosophila*. Ost-A will only transfer completed glycans, while Ost-B is permissive, and will transfer glycans with missing residues (Ruiz 2008). Because *alg10* acts late in the pathway, Ost-B is predicted to transfer the largely completed glycans to their target proteins, allowing for partial glycosylation, while the partially complete oligosaccharide produced by *alg9* mutants produce glycans incapable of transfer, leaving target proteins completely unglycosylated.

1.3 Congenital disorders of glycosylation

A family of human genetic disorders called the congenital disorders of glycosylation (CDG) are caused by mutations in the N-linked, as well as the related O-linked, glycosylation pathways. Of the group of over 80 identified disorders, 24 are caused by defects in the assembly of N-glycans, 27 are due to errors in glycan processing, 19 are linked to the O-linked glycosylation pathway, and still others fall under the classification of CDG-x for a disease with unidentified defects (Jaeken,

2015). In the above Figure (1.1) the genes labeled in red are those that have been documented in a CDG cases, those in blue have not.

Clinical presentations of these disorders vary greatly, but most involve some degree of nervous system defect resulting in ataxia, hyporeflexia, and developmental delays (Jaeken 2014). Because of the high degree of variability in symptomatic presentation, it is likely that CDGs are far more common than currently understood. There is no published data on the prevalence of CDGs, but the most common form of CDG, Pmm2-CDG (CDGIa), has been identified in more than 700 individuals (Jaeken 2015). The mortality rate for infants born with CDG is 20% within the first year of life. Though there is now clinical testing for over 30 CDG related genes, there are no current treatments available to CDG patients (Jaeken 2014).

Table 1.1 An identified CDG exists for almost every gene associated with the N-linked pathway. The genes and related disease relevant to this study are highlighted in yellow. The phenotypes of these diseases are pleotrophic and often difficult to diagnose (adapted from Jaeken 2014).

Name	Main clinically affected organs and systems	Defective protein	Defective gene
CDG-Ia	Nervous system, fat tissue, other organs1	Phosphomannomutase 2	PMM2
CDG-Ib	Intestine, liver	Phosphomannose isomerase	MPI
CDG-Ic	Nervous system	Glucosyltransferase I	hALG6
CDG-Id	Nervous system	Mannosyltransferase VI	hALG3
CDG-Ie	Nervous system	Dolichol-P-Man synthase I	DPM1
CDG-If	Nervous system, skin	Lec35	Lec35
CDG-Ig	Nervous system	Mannosyltransferase VIII	hALG12
CDG-Ih	Intestine, liver	Glucosyltransferase II	hALG8
CDG-Ii	Nervous system, eyes, liver	Mannosyltransferase II	hALG2
CDG-Ij	Nervous system	UDP-GlcNAc: dolichol phosphate,	DPAGT1
CDG-Ik	Nervous system, liver	Mannosyltransferase I	hALG1
CDG-Il	Nervous system, liver	Mannosyltransferase VII/IX	hALG9

CDG-IIa	Nervous system, skeleton, intestine, immune system, dysmorphism	N-acetylglucosaminyltransferase II	MGAT2
CDG-IIb	Nervous system, dysmorphism	Glucosidase I	GLS1
CDG-IIc	Nervous system, immune system, dysmorphism	GDP-fucose transporter 1	FUCT1
CDG-IId	Nervous system, skeletal muscles	-1,4-galactosyltransferase 1	B4GALT1
CDG-IIe2	Nervous system, liver, skeleton	Conserved oligomeric Golgi complex, subunit 7	COG7
CDG-IIf	Megathrombocytopenia, neutropenia	CMP-sialic aid transporter	SLC35A1

1.4 The Unfolded Protein Response (UPR)

In studies of *alg5,* a gene coding for an enzyme that acts in between *alg9* and *alg10* in the N-linked pathway, induction of a process called the unfolded protein response (UPR) was found (Shaik et al. 2011). The UPR is a three pronged pathway that is activated in response to intracellular stress caused by an excess of unfolded or misfolded proteins in the ER. This pathway has three purposes, to promote cell survival by downregulating global transcription, to reduce protein load in the ER and upregulate translation of chaperone proteins, and to trigger cell death upon prolonged stress induction (Tabas 1011).

This project highlights one pathway in particular, the IRE1 dependent pathway. XBP1 is a constitutively produced mRNA that requires processing by IRE1 in order to be translated (Calfon et al 2002). XBP1 then acts as a transcription factor for chaperones that assist in protein folding process.

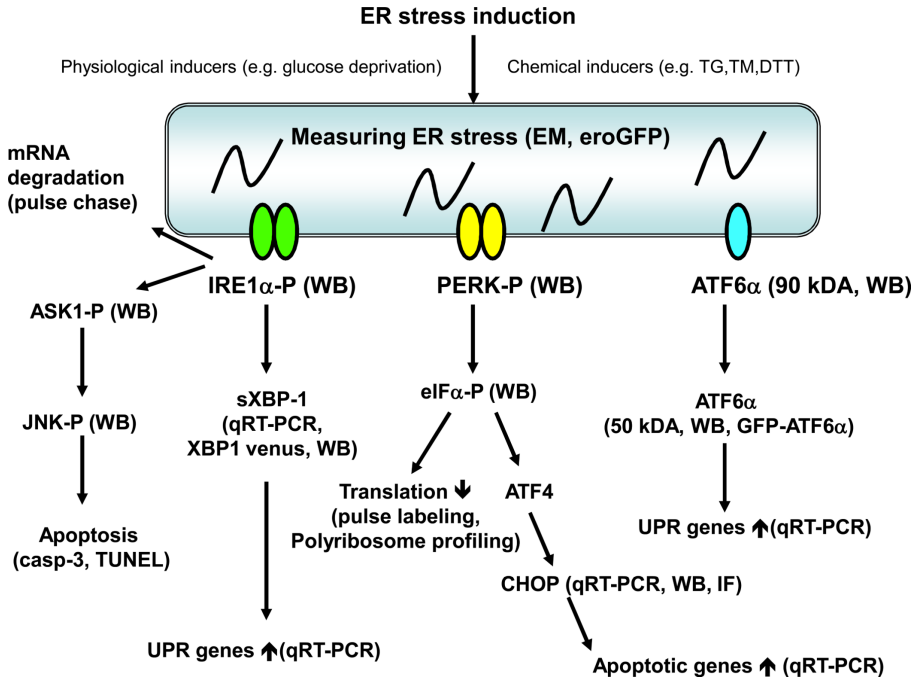

Figure 1.2 The UPR pathway is mediated by three sensor proteins IRE1, PERK and ATF6. Each sensor protein stimulates an independent pathway in an attempt to correct ER stress. (Oslowski et al 2011)

1.5 *Drosophila* as a Model

Since the discovery of sex-linkage by Thomas Hunt Morgan in the beginning of the 20th century, *Drosophila* has become the model organism of choice for many geneticists. *Drosophila* offer many advantages over other models that make the fruit fly an attractive choice for study. The fruit fly combines the cost effective nature and relatively short generation time and sophisticated genetics with the ability to study complex systems allowed by higher organisms, as well supportive cell culture models.

Drosophila undergo four distinct developmental stages. The embryonic stage lasts less than 24 hours and is quickly overtaken by the first of three larval stages. The 1st and 2nd instar larval stages each last about one day, with the 3rd instar lasting two days. After the 3rd instar, pupa form as the final developmental stage before adulthood.

After 4 days adult flies emerge (Figure 1.3). With a typical generation time (embryo to adult) of ten days at room temperature, rearing many generations of *Drosophila* is far less time consuming than a mammalian model, such as mice, which require a gestation period. The fruit fly also produces far more progeny per generation, resulting in more offspring of the desired genotype per generation. Though, with so few hours spent in each distinct developmental stage, timing experiments to the proper developmental stage of the fly can be difficult.

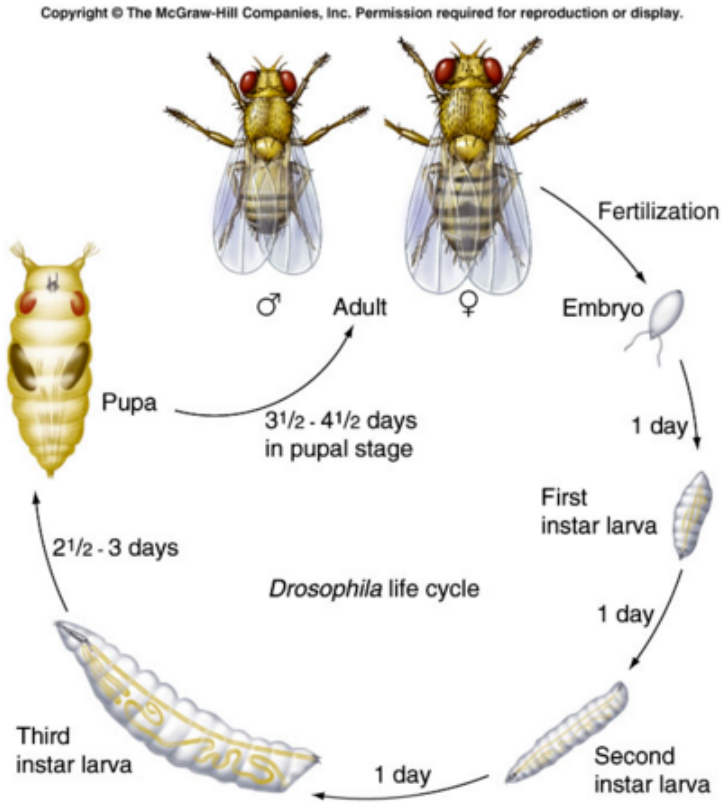

Figure 1.3 The *Drosophila* lifecycle is divided into four separate phases: embryo, larval, pupal and adult. Flies of the third instar larval and the adult stages were used in this study (Hartwell, 2006).

Another distinct advantage of using *Drosophila* as a model system is the ability to suppress random recombination events through use of balancer chromosomes. Balancer chromosomes have three distinct features: the presence of several inversions that suppress recombination, a recessive lethal marker, and a dominant phenotypic marker. The suppression of recombination events preserves placement of transgenic elements and mutations in the *Drosophila* genome, and ensures that any identified genetic components stay where they are known to be. Several dominant phenotypic markers are used to indicate by observation whether or not a balancer chromosome is present in a given specimen. By putting a mutation over a balancer chromosome, one can always be certain whether a fly is homozygous for their mutation because these specimens will lack the dominant phenotypic marker.

The recessive lethal marker on balancer chromosomes allows the generation of self-maintaining stocks, that is to say, stocks that maintain the same genotype in every progeny from generation to generation. In this way a mutation can be maintained in a heterozygous state over a balancer chromosome indefinitely.

1.6 *Drosophila* eye development

The development of the *Drosophila* eye is well defined and highly ordered, making it a perfect model tissue in which to study developmental pathways. It is also a tissue non-essential to life, so homozygous lethal mutations can be expressed in a mosaic manner in the eye tissue only, allowing for study of the specimen at all points of development while circumventing the lethal phenotype.

The *Drosophila* eye is a compound eye made up of over 750 highly ordered facets called ommatidia (Figure 1.4A). Each ommatidium is made of eight photoreceptor cells that arise from the sequential division of a single progenitor

neuron (Figure 1.4B). The central R8 cell differentiates first. Then photoreceptor cells differentiate in a pairwise fashion. First, R2 and R5, R3 and R4, and R1 and R6. R7 is the last photoreceptor to develop distinct character and is also the only UV sensing cell of the ommatidia (Figure 1.4 C and D). All of this development takes place in the third instar larval stage in the eye imaginal disc. Ommatidia develop posterior to anterior along what is called the morphogenetic furrow (Figure 1.4C). Because of this, the age of the imaginal eye disc can be easily determined, which can be useful in determining whether observed phenotypes are age dependent.

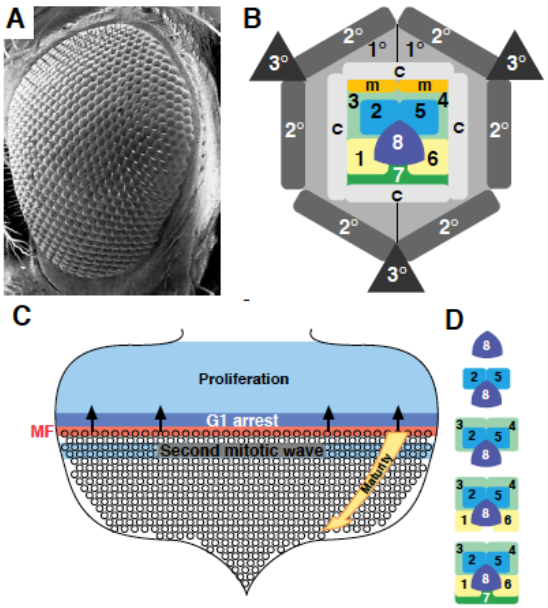

Figure 1.4 A) The adult *Drosophila* eye is made up of over 750 lenses. B) Illustration of the ommatidial cluster including photoreceptors and support cells. C) Development of the ommatidia within the 3rd instar larval imaginal eye disc (anterior is up) D) Differentiation of photoreceptor cells within the ommatidia (Freeman 1997).

1.7 Purpose and Specific Aims

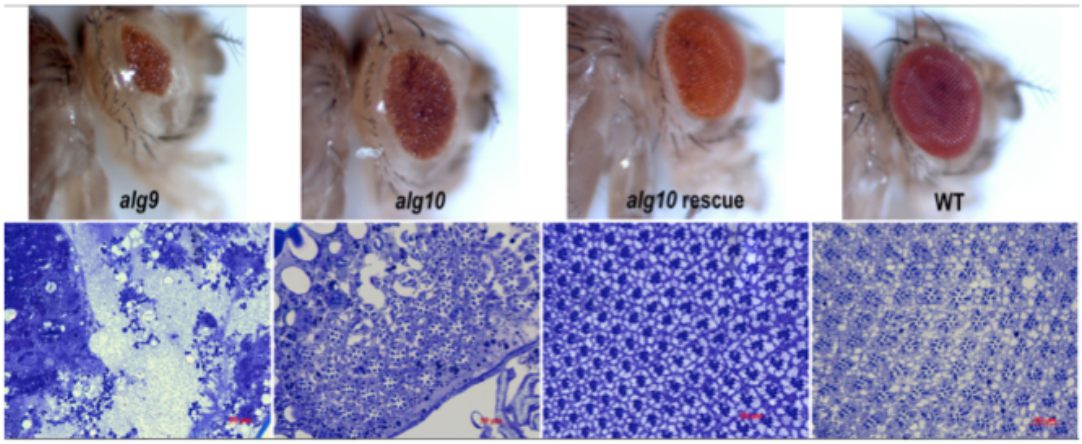

Figure 1.5 **:** Top: Rough eye phenotypes observed in adult eyes. Bottom: Light microscope images of toluidine blue stained plastic sections of adult eyes (adapted from McCague, 2013).

Previous studies have revealed defects in cuticle formation in the embryonic stage and a rough eye phenotype (Figure 1.5) in adult flies as a consequence of *alg 9* and *alg10* homozygous mutations (McCague 2012). The purpose of this study is to characterize the effects of *alg9* and *alg10* mutation in the developing eye disc. It is hypothesized that defects in the adult eye are caused by underglycosylation of target proteins in the ER. The interruption in the N-linked pathway leads to improper trafficking of glycoproteins and intracellular stress. Possible induction of the unfolded protein response (UPR) will be studied, as it's involvement in other CDG models has been noted (Shaik et al. 2011). The specific aims of this project are:

Specific aim 1: Examine protein targets of the N-linked glycosylation pathway in the eye imaginal disc of *alg9* and *alg10* mutants.

Specific aim 2: Characterize differences in neuronal organization between the wild type and *alg9* and *alg10* mutant eye discs.

Specific aim 3: Determine the molecular reason(s) for the defects seen in the *alg9* and *alg10* mutant eye discs.

Specific aim 4: Show that expression of *alg10* rescues the phenotype created by the knockout model.

Chapter 2

METHODS

2.1 Stocks and stock maintenance

Stocks were maintained in vials containing a food medium (yeast, agar, cornmeal and glucose), Carolina™ blue food, and yeast at room temperature in mild humidity with 12 hour interval light/dark cycles. As stocks were expanded flies were moved into bottles containing the same food medium, Carolina™ blue food, and yeast to increase yield of larva and virgins. Bottles containing flies at the pupal stage were moved to storage at 18°C to slow the hatching process to allow more time to collect virgins to be used in crossing experiments. Stocks kept in vials at room temperature were maintained as backups and were flipped into fresh vials every 10-12 days. Virginable stocks in bottles or vials were flipped into fresh bottles every 4-6 days. Stocks were checked regularly for mites and mold to ensure the health and viability of the flies. The genotypes of the stocks maintained are listed in the table below.

Table 2.1 Genotypes of all balanced stocks maintained for use in experiments. Virgin females and young males were used from each stock to create experimental crosses.

w/w;ey-Gal4 UAS-Flp/SM5;gmr-hid FRT^{2A}*/TM6B*	*w/w; alg10-10*FRT^{2A}*/TM6B*
w/w: ey-Gal4 UAS-Flp / ey-Gal4 UAS-Flp; FRT^{82B} *gmr-hid/TM6C*	*w/w; Sp/CyO;* $FR82^{8B}$ *alg9/TM6C*
w/w;UAS-alg10/CyO; alg10-10 FRT^{2A}*/TM6C*	*w/w; UAS-xbp-gfp /CyO;* FRT^{82B} *alg9/TM6C*
w/w; UAS-xbp1-gfp /CyO; alg10-10 FRT^{2A}*/TM6B*	

2.2 Virgin collection and genetic crosses

Virgins were collected daily during the academic year and twice daily during summers from bottles stored at 18°C. Bottles kept at 18°C were discarded after one month. During the collection process flies were anesthetized using CO_2 and were sorted using a paint brush under a dissection microscope on a CO_2 pad to maintain immobility for ease of sorting. Virgins were kept in separate vials at 18°C for no more than 3 days until enough were collected to create a cross. Males of the appropriate genotype were selected in a similar manner. Experimental crosses were maintained in vials stored at room temperature and flipped every four days.

2.3 Generating genetic mosaics

In order to circumvent the embryonic lethal phenotype of the *alg9* and *alg10* homozygous knockout, the ey-Flp method was used to create genetic mosaic flies expressing homozygous *alg9* and *alg10* mutations in the eye tissue only through mitotic site specific recombination. Expression of the mutant genes is controlled by the UAS-GAL4 expression system in conjunction with FLP/FRT recombination. UAS-GAL4 is a transgenic system commonly used to control spatial and temporal expression of target genes in the *Drosophila* genome (Figure 2.12). The system consists of two parts, a GAL4 driver line and a UAS site. GAL4 is a trans-acting transcription factor that binds to Upstream Activator Sequences (UAS) located upstream of target gene to activate transcription. By placing GAL4 expression under the control of a tissue specific promoter, in this case *eyeless (ey)*, which promotes

expression in developing eye tissue, genes downstream of the UAS site can be selectively activated in specific tissues (Brand 1993).

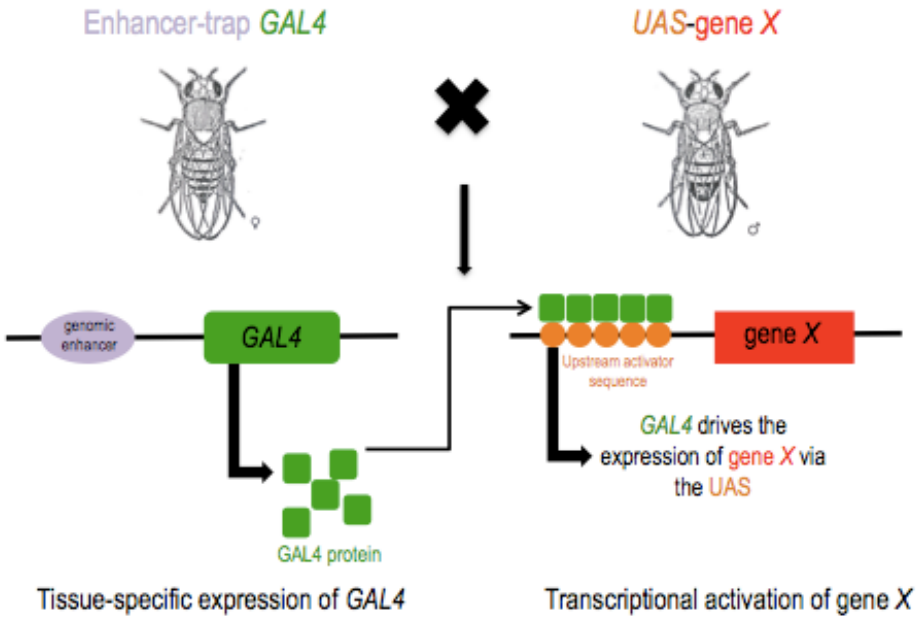

Figure 2.1 UAS-GAL4 is a transgenic tool native to yeast that allows special and temporal control of gene expression. In this study expression of FLP was controlled using this mechanism (Figure adapted from St. Johnson, 2002).

FLP, a site-specific recombinase, is placed under the control of the UAS sites and ultimately causes recombination between homologous chromosomes at FRT target sequences in the eye tissue only, resulting in homozygous mutant eye tissue in an otherwise heterozygous background (Beumer KJ 1998).

Cells not homozygous for the *alg9* or *alg10* mutation were eliminated using the dominant lethal gene GMR-hid. GMR is another eye specific promoter that drives the expression of the pro-apoptotic gene *hid*, a dominant lethal gene, in the eye tissue

only (Song 2000). In this way, only cells homozygous for the mutation, lacking a single copy of *hid*, will survive (Figure 2.2).

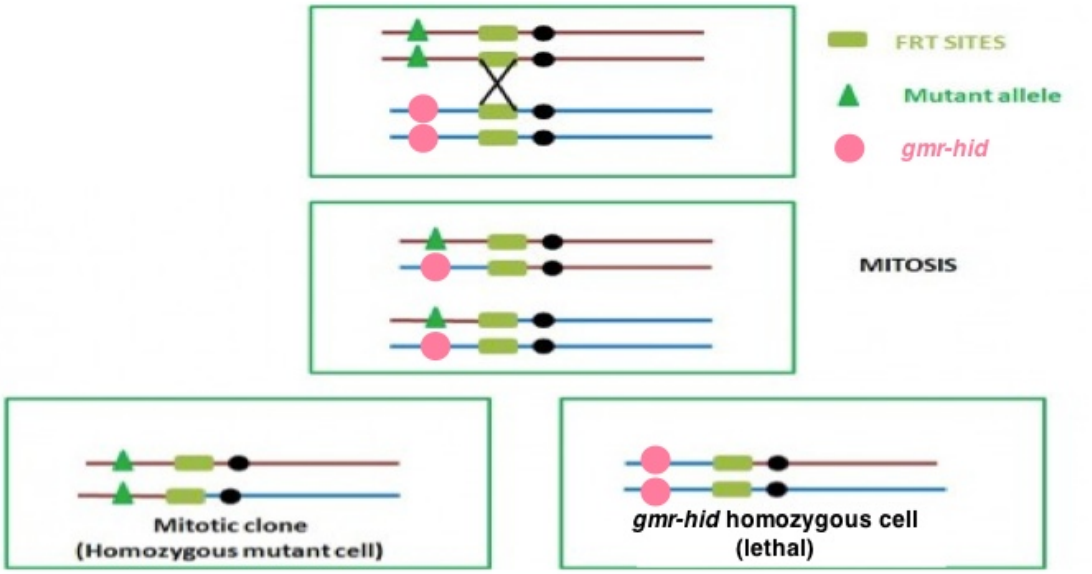

Figure 2.2 Gene expression was controlled using the *ey-Flp gmr-hid* system. Through site specific recombination, this results in eyes composed of homozygous mutant tissue in an otherwise heterozygous background.

2.4 Imaginal disc collection and dissection

In order to study the affects of the *alg9* and *alg10* mutations on eye development, eye imaginal discs were extracted from the third instar larva. Crosses used to generate the proper larval genotype are outlined in Appendix A.

Imaginal discs were dissected from third instar larva after they began to crawl up the sides of their vials, indicating they were old enough to contain well-developed discs. Larva of the correct phenotype, lacking the balancer phenotype *Tb*, which generates shorter bodied larva, were collected. The long body (non-*Tb*) phenotype indicated larva containing the mutant chromosome and the *gmr-hid* chromosome capable of undergoing homologous recombination to yield homozygous mutant eye tissue (Figure 2.2, second panel down). Primary dissection to remove excess cuticle and fat body from the larval sample was performed in cold phosphate buffered saline (PBS) solution under a dissection scope. Samples were placed in 1.5mL centrifuge tubes on ice until completion of dissections. After completion of the primary and secondary staining protocol, a secondary dissection was performed to isolate the disc of interest (eye or wing, Figure 2.3) Discs were mounted on slides using 70% glycerol/PBS medium. Exact dissection method followed the steps outlined in Purves, D. C., *et. al* (2007).

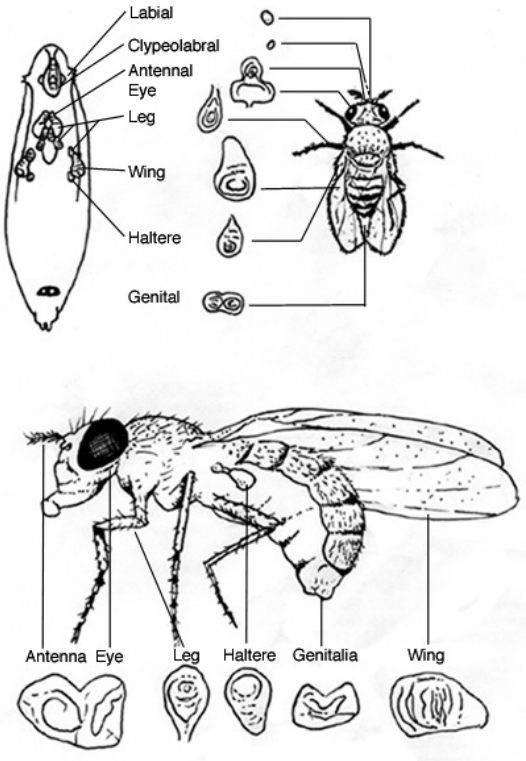

Figure 2.3 The third instar larva contains several imaginal discs that develop into adult features. The disc of interest in this study was the eye imaginal disc located behind the mouth hooks of the larva and attached to the lobes of the immature brain. Wing discs were dissected also for use as a control in some experiments (adapted from Cruz, 1993).

2.5 Imaginal disc staining

Primary staining of selected imaginal discs was performed after primary dissection of the larva. Discs were first fixed in 4% formaldehyde 1X PBS for 20 minutes at room temperature. Samples were then washed four times for 5-10 minutes each in cold PBT (PBS with 0.5% Triton-X100). After washing, the discs were blocked for 30 minutes at room temperature in PBTN (PBT with 5% normal horse serum). Staining was the performed on a rocker in PBTN for two hours at room

temperature or at 4°C overnight. A list of antibodies and their dilutions is provided in Appendix B.

Primary staining was followed by another round of four, 5-10 minute washes in PBT. Secondary staining took place in PBTN with various fluorescently labeled secondary antibodies at a concentration of 1:500 at room temperature for one hour. After both stainings were completed, secondary dissection took place to isolate stained discs. Fully stained eye discs were visualized with a Zeiss LSM 780 confocal microscope and images were captured using Zen imaging software. Complete slides were stored in a light protective folder at 4°C.

2.6 Western blot analysis

Western blot was used to examine the total eye tissue present in the adult eye as well as to look at the molecular weight of target proteins of the N-linked pathway. Eye tissue samples for western blot analysis were collected from adult fly heads. Adult flies homozygous for the *alg9* and *alg10* mutations were recognized by the rough eye phenotype, separated, and immobilized on a CO_2 pad. A razor blade was then used to separate the head from the body. Because the adult eye is embedded deeply in the adult head, further isolation of the eye tissue was avoided. The heads were placed in sample buffer (62.5 mM Tris-HCl pH 6.8, 2.5 % SDS, 0.002 % Bromophenol Blue, 0.7135 M (5%) β-mercaptoethanol, 10 % glycerol) and homogenized using 30 strokes 3x with a 30 second spin in the centrifuge between rounds of homogenization. After the final round of homogenization samples were spun for 1 minute and 30 seconds and then heated to 75°C for 3 minutes. Samples were then loaded on a 15% acrylamide gel and run for 6 hours at room temperature. Protein on the gel was transferred to a

nitrocellulose membrane overnight at 4°C using a 20 Volts current in a transfer buffer (25 mM Tris, 190mM glycine, 20% methanol).

The following day the membrane was blocked in Tris buffered saline Tween 20 (TBST) 5% milk for 1 hour at room temperature. Blocking solution was removed and various TBST diluted antibody solutions were applied for 1 hour at room temperature. After staining the primary staining solution was removed and stored at 4°C. The membrane was then washed 3X for 15 minutes each in TBST at room temperature. Secondary staining with various HRP conjugated antibodies took place for one hour at room temperature. After secondary staining the membrane was again washed 3X for 15 minutes each at room temperature. Amersham ECL Western Blotting Detection Reagent solutions were applied to the membrane 5 minutes prior to visualization with the FlourChem Q Imaging System.

2.7 Genetic rescue of *alg10*

It is important when creating a genetic knockout model to ensure that any observed phenotype that arises is a result of the knockdown of the intended protein, and not from unintended extraneous consequences of other mutations on the FRT chromosome. Demonstrating that re-expression of the target protein can rescue the mutant phenotype, the eye to wild type morphology, acts as a control that demonstrates successful knockdown. In order to demonstrate this rescue, a line of flies containing both the knockdown of the *alg10* gene and an insertion of wild type *alg10* under the control of UAS-GAL4 was generated. Crossing of this stock with a balanced driver line resulted in flies that expressed wild type *alg10* under the control of the UAS promoter in the background of the *alg10* knockout eye.

2.8 XBP1-GFP assay

The UPR is a three pronged pathway that is activated in response to intracellular stress caused by an excess of unfolded or misfolded proteins in the ER (Tabas 2011). There are several markers of UPR that can be used to study its induction. As explained in section 1.4, interaction of IRE1 and XBP1 occurs upon induction of UPR (Figure 2.4).

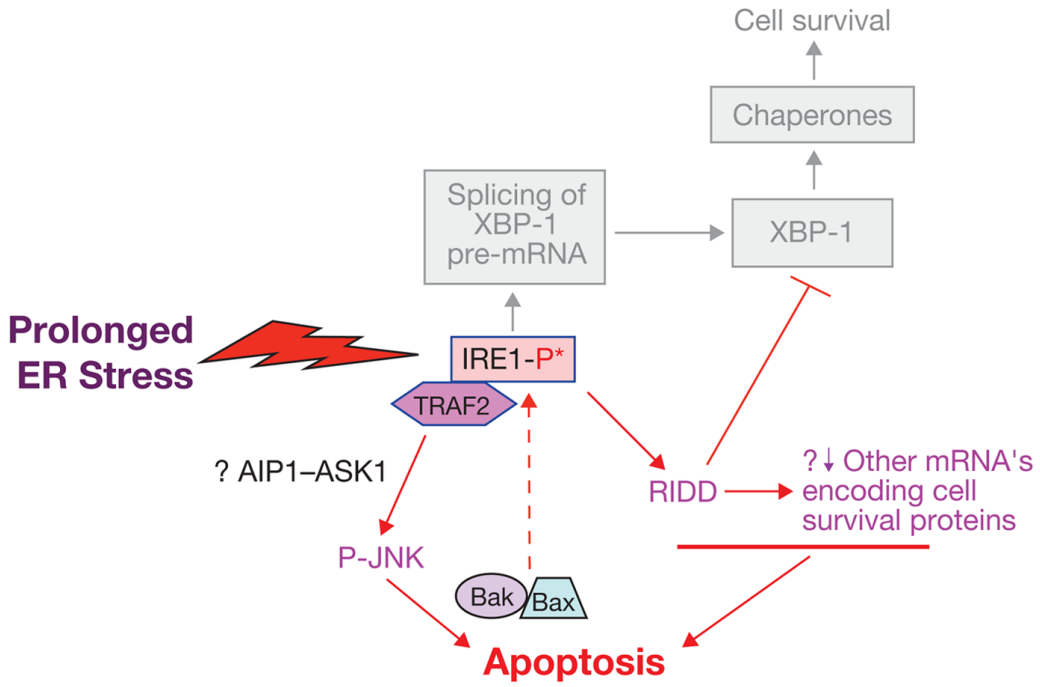

Figure 2.4 The IRE-1 dependent pathway of the UPR has two actions, the first is to splice XBP1 pre-mRNA into its translatable form. This action promotes cell survival. When prolonged stress occurs, IRE-1 activity switches to phosphorylate JNK, triggering a pro-apoptotic cascade (Tabas 2011).

In order to take advantage of this conditionally translated protein, *Ryoo et. al* developed an *UAS-xbp1-gfp* expressing *Drosophila* line to examine the induction of

UPR (Figure 2.5). Upon induction of UPR, XBP1 containing a green fluorescing protein (GFP) tag will be spliced by IRE-1 and translated into full-length protein tagged with GFP. Thus, cells marked with GFP are undergoing UPR. This study used this expression construct in conjunction with the *alg9* and *alg10* knockdown lines to examine induction of UPR as a result of N-linked glycosylation defects.

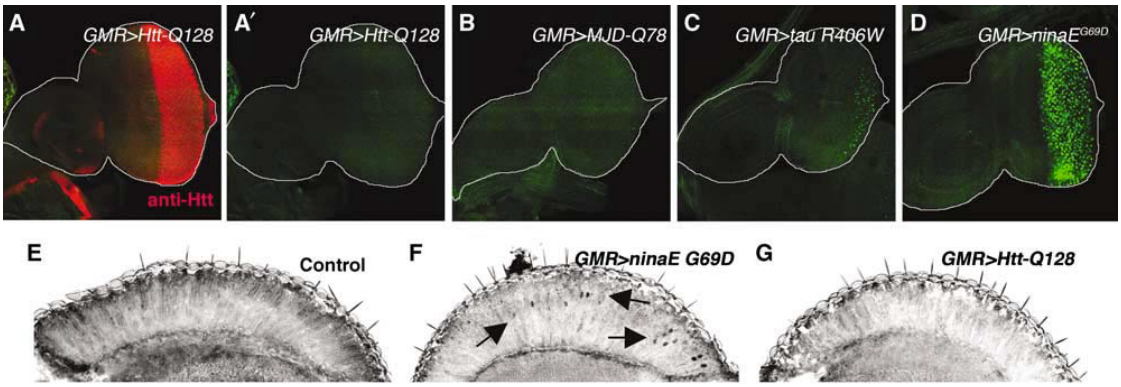

Figure 2.5 XBP1-GFP expressing construct indicates successful induction of UPR. GFP expressing cells are experiencing intracellular stress and induction of UPR (Ryoo *et. al* 2007).

In order to establish a positive control, primary dissection of eye and wing discs was done according to the methods in section 2.4. After primary dissection tissue was placed in Schneider's media (Gibco) containing 0.1M DTT to induce ER stress and UPR. Discs then underwent normal fixing, blocking, staining and mounting protocols. Discs were stained for Wingless, ELAV, and GFP.

Chapter 3

RESULTS

3.1 *alg9* and *alg10* eye discs show organizational irregularities

Eye disc stainings and mounts were created using the method outlined in sections 2.4 and 2.5. ELAV, embryonic lethal abnormal visual system, is a neuron specific protein that is expressed in all neurons at all stages of development (Robinow *et. al*, 1991). This protein was used as a pan-neuronal marker *in vivo* to visualize the general organization of the ommatidia in the imaginal disc. Wide type eye discs show a highly organized pattern of development, maturing in clear rows from posterior to anterior of the tissue following the morphogenetic furrow (Figure 3.1 and 3.2, top panels green). *alg10* mutants show a slight breakdown of this overall structure, with ommatidia beginning to crowd one another. *alg9* mutants show a much more severe phenotype with some ommatidial clusters crowding one another and others spreading out (Figure 3.1 and 3.2, top panels green). Successful staining with ELAV indicates that the photoreceptors of the mutant eye are still acquiring neuronal character, despite the mutations.

Another distinct feature of the mutant eye tissue is the absence of one or more photoreceptors in some of the ommatidial clusters. In the wild type samples, each ommatidium takes on a distinctive flower shaped cluster indicating that all photoreceptors are present. In both the *alg9* and the *alg10* mutants younger ommatidia resemble that of the wild type ommatidial clusters; however, in ommatidial clusters nearest to the posterior face of the disc, which are also developmentally the oldest

ommatidia, are missing individual photoreceptors (Figure 3.2, top panels green). This indicates age related cell loss is occurring later in development.

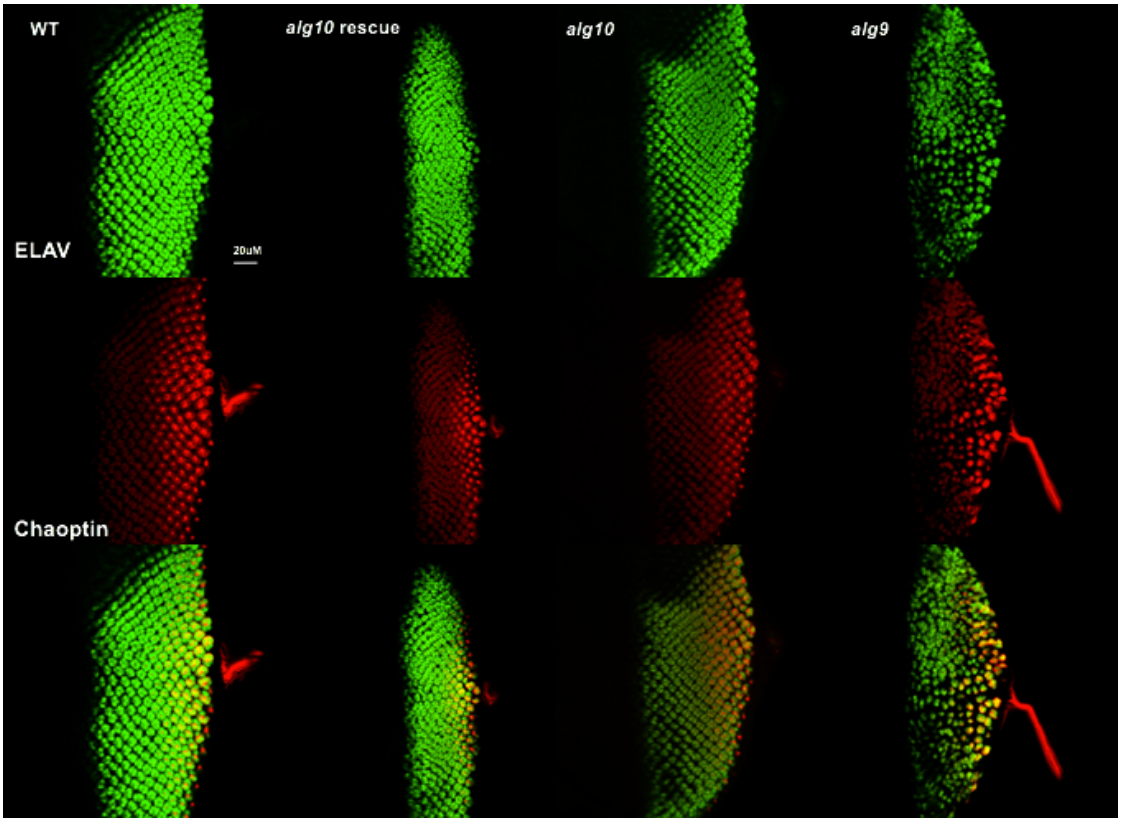

Figure 3.1 ELAV (green) is a pan-neuronal marker used to show the general organization of the ommatidia in the eye disc, green (top panels). Chaoptin (red, middle panels) is a cell surface axonal glycoprotein. The lower panels show the merged images. Images are organized anterior, right and posterior, left. *alg9* and *alg10* eye discs show retention of glycoprotein in the cell body. The lower panel shows merged images. In all images eye discs are oriented anterior right and posterior left.

In addition to the organizational phenotype revealed by ELAV staining, stainings of target proteins of the N-linked glycosylation pathway revealed improper

trafficking of these proteins and accumulation of protein in the cell body. Each of the eight photoreceptor cells of an ommatidium contains a photosensitive element called a rhabdomere, which is located at the center of the cluster. Chaoptin, an axonal glycoprotein responsible for cell-to-cell adhesion between membranes in the microvilli of photoreceptors around these rhabdomeres (Van Vactor *et. al*, 1988), was used to visualize the effects of improper glycosylation on a target protein of the N-linked pathway (Figure 3.1 and 3.2, middle panels, red).

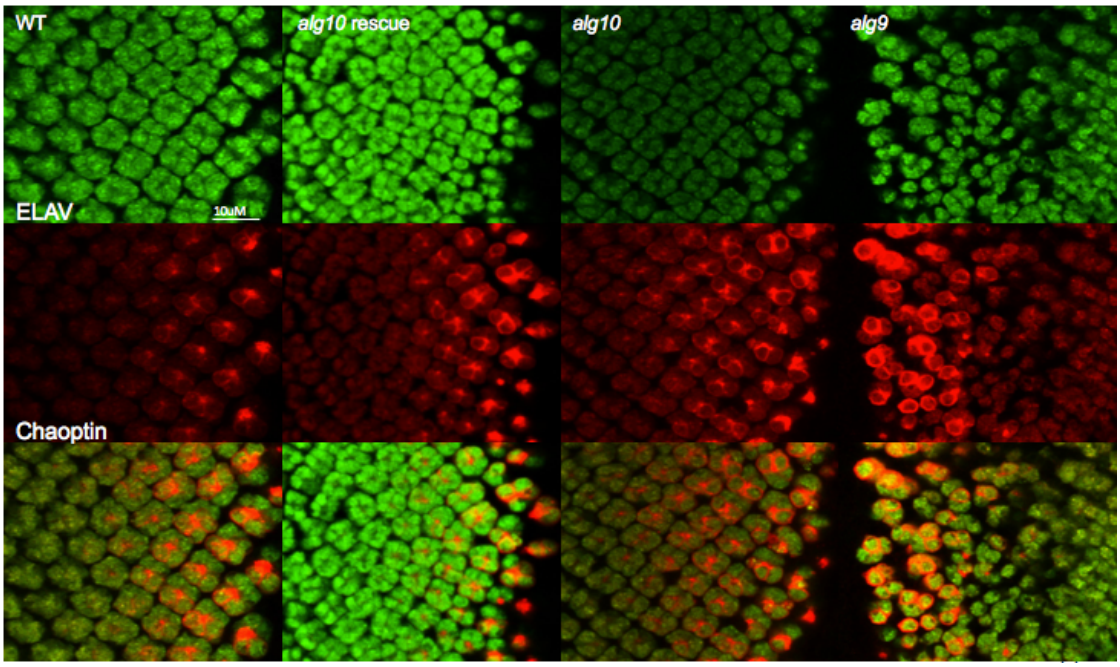

Figure 3.2 Chaoptin (red) is a cell surface axonal glycoprotein that is normally localized in the axon. Both *alg9* and *alg10* mutants show retention of Chaoptin in the cell bodies. The *alg10* rescue shows localization of Chaoptin similar to the wild type control. ELAV is in green (top panels) and Chaoptin (red, middle panels). The lower panels show the merged images.

As expected, localization of Chaoptin in the wild type disc is to the center of the ommatidial cluster where the rhabdomeres, and the microvilli surrounding them, lie. As a result of *alg9* and *alg10* mutation Chaoptin is found in improper locations. In both *alg9* and *alg10* mutants, Chaoptin is retained in the cell bodies and is no longer oriented toward the center of the ommatidial cluster (Figure 3.1 and 3.2, middle panels, red). *alg9* presents with a much more severe phenotype. This buildup appears to increase over time, as the oldest cells near the posterior edge of the eye disc show the greatest levels of retention (Figure 3.2, middle panels, red).

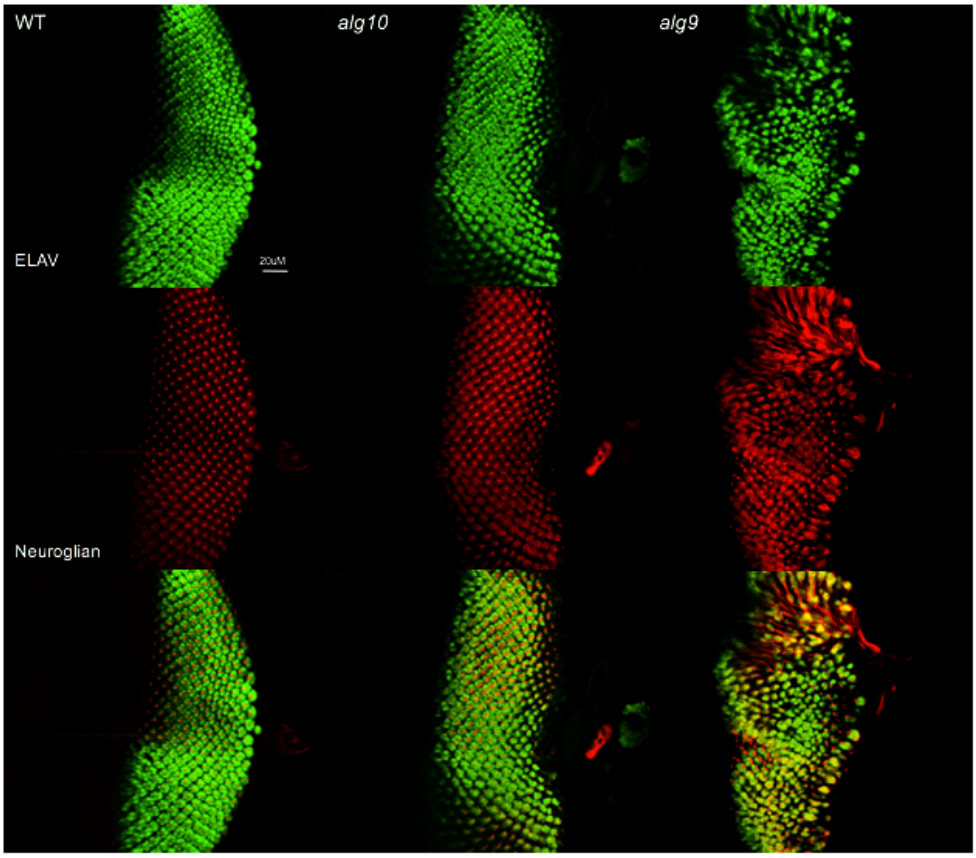

Figure 3.3 **:** Neuroglian, an integral membrane protein from the immunoblobulin super family, is retained in the cell bodies of *alg9* and *alg10* mutant eye discs. Normal localization patterns are to the membrane of both cell bodies and axons. ELAV is in green (top panels) and Neuroglian (red, middle panels). The lower panels show the merged images.

Neuroglian, another target of the N-linked pathway was also studied. Neuroglian is an integral membrane glycoprotein that is present in many neuron types including photoreceptors. This protein has localization to membranes associated with the cell body as well as to the length of the axons that leave the ommatidial cluster (Beiber *et. al*, 1989). Similar to the phenotype observed in the Chaoptin stainings, Neuroglian shows differences in localization as a result of *alg9* and *alg10* mutation.

Wild type Neuroglian is visualized as a small puncta at the center of the ommatidial cluster, presumably at the point where the axons of the cluster meet and project backwards to the optic nerve. Both mutants lose this tight localization and again show retention in the cell body. Mirroring the results of all prior experiments, *alg9* presents with an increased severity of phenotype (Figure 3.3).

3.2 *alg9* and *alg10* eye discs show loss of axon adhesion and pathfinding

Further study of Neuroglian in the axons of the developing eye disc revealed loss of axonal organization in mutants. Examination of the optic nerve (Figure 3.4) of wild type discs shows tight bundling of axons at the midpoint of the posterior side of the eye disc. The axons then extend back towards the brain lobes. Both mutants show a spreading of these axons into a wild mass rather than an organized tract.

Many glycoproteins act as cell-to-cell adhesion molecules. Improper glycosylation may be affecting the ability of axons to adhere to one another in two ways. First, as seen with Chaoptin, glycoproteins involved in axonal adhesion may be sequestered in the cell body as a consequence of under-glycosylation, leading to fewer adhesion molecules at the cell surface. Second, adhesion molecules that do reach their proper positioning will contain improperly formed and processed glycans. Having not undergone proper trimming and modification of the glycan that extend into the extracellular matrix, it is possible that even glycoproteins that do make it to the cell surface are incapable of interacting with one another to form adhesion sites.

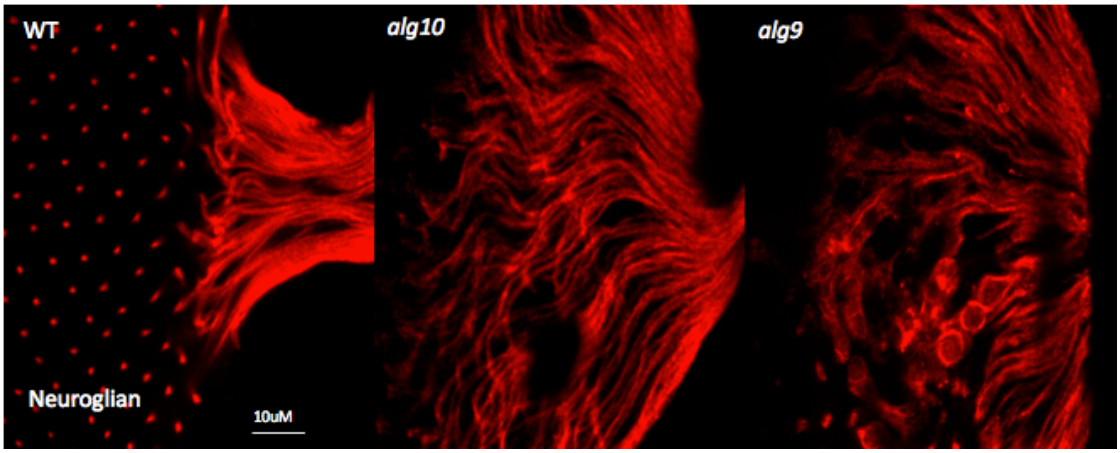

Figure 3.4 Axons leaving the eye disc via the optic stalk in the eye imaginal disc adopt a high level of organization (WT). This organization is disrupted in *alg9* and *alg10* mutant eyes. Neuroglian is shown in red. Neuroglian shows localization to both the axons and body of neural cells. In the mutant samples, axons exiting the eye disc through the optic nerve show decreased levels of organization.

3.3 *alg9* and *alg10* eye discs show elevated levels of apoptosis

In Figure 3.2, it was noted that older ommatidial clusters in the eye discs seemed to be missing individual photoreceptor cells. This discovery warranted investigation into the possibility that apoptosis was occurring in an age related manner. Antibody staining against cleaved caspase 3, a protein that is cleaved as part of the apoptotic signaling cascade, revealed elevated levels of caspase 3 cleavage in both *alg9* and *alg10* mutants (Figures 3.6 and 3.7). Wild type discs showed no indication of apoptotic induction. This mass induction of apoptosis as the photoreceptor cells age may account for the rough eye phenotype observed in adult mutants, and is also likely responsible for the reduced levels of functional eye tissue present in most mutants.

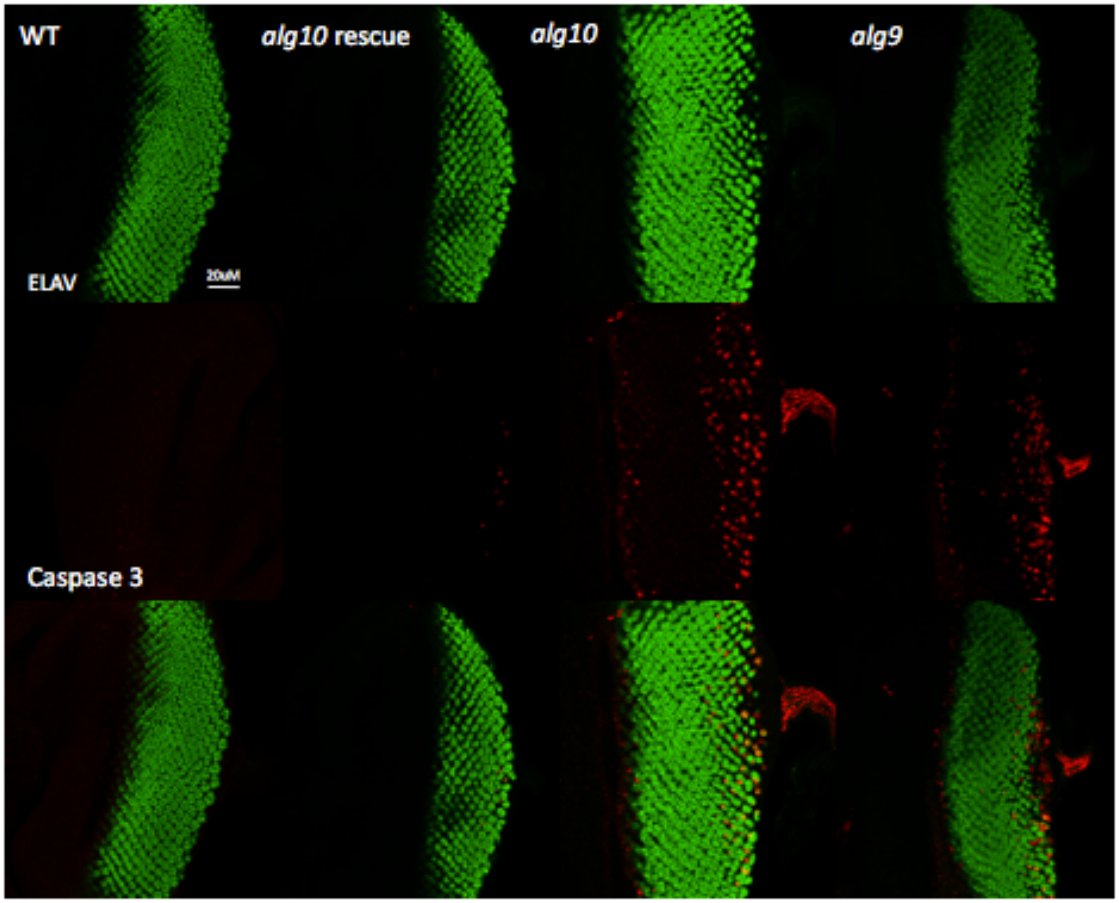

Figure 3.6 Cleaved Caspase-3 is a marker of apoptosis. Both mutants show a significant increase in apoptosis compared to wild type. The *alg10* rescue shows reduced apoptosis. ELAV is in green (top panels) and cleaved caspase (red, middle panels). The lower panels show the merged images. In all images eye discs are oriented anterior right and posterior left.

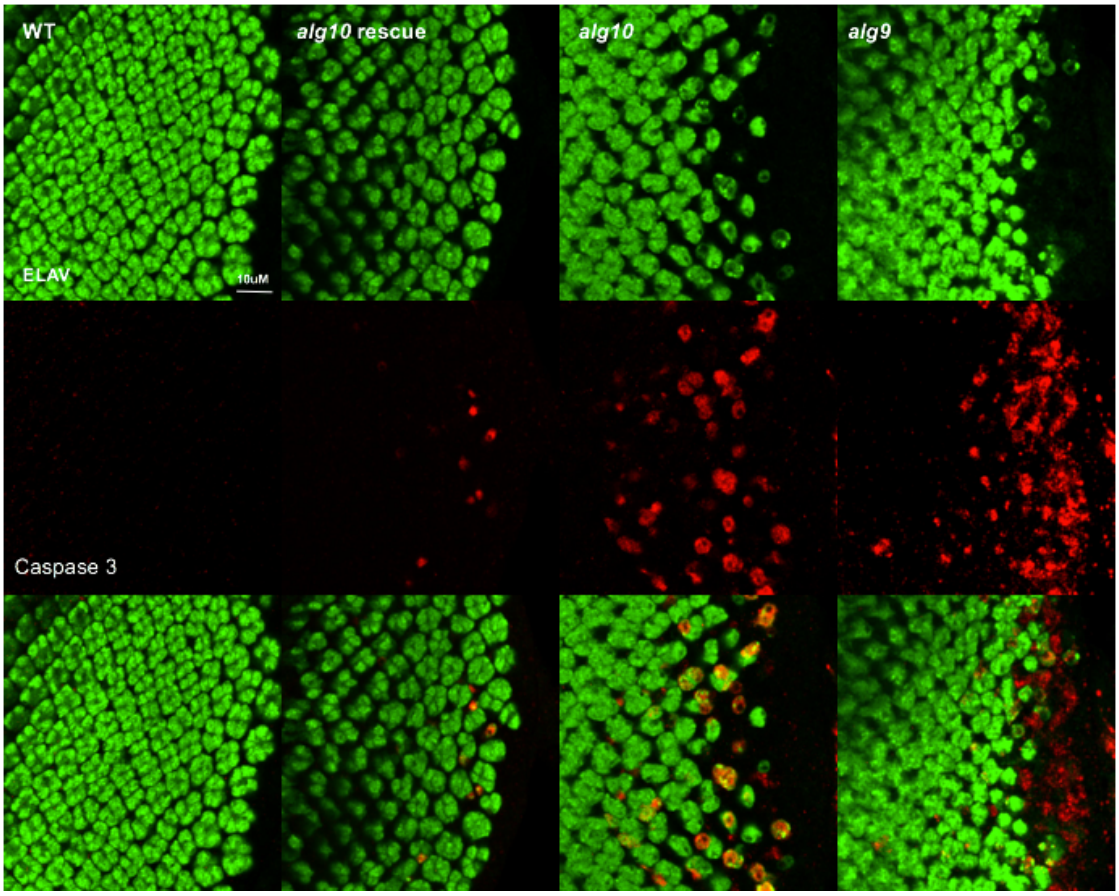

Figure 3.7 Caspase 3 staining indicates individual cells from each ommatidial cluster undergo apoptosis. All apoptotic events occur on the posterior edge of the eye disc where the oldest photoreceptors lie. ELAV is in green (top panels) and cleaved caspase (red, middle panels). The lower panels show the merged images. In all images eye discs are oriented anterior right and posterior left.

3.4 Expression of Alg10 rescues viable eye tissue

In the immunofluorescent staining experiments, re-expression of *alg10* in the background of the *alg10* knockout model caused improvement of the mutant phenotype (Figures 3.1 and 3.2). These discs show reduced levels of apoptosis compared to both the *alg9* and the *alg10* mutants (Figures 3.6 and 3.7) and it was

found in prior studies in the Selva lab, that expression at *alg10* rescues the rough eye phenotype in adult eyes (Figure 1.5 McCague, 2012). Through western blot analysis, it was shown that rescue with functional *alg10* produces adult eyes with comparable amount of functional eye tissue when compared to wild type adults. Rhodopsin, an eye specific photopigment, was used as a marker to quantify total eye tissue. Rhodopsin is also an N-glycosylated protein in its immature form, and it's glycosylation is removed once it reaches the cell membrane (Katanosaka, 1998). This comparison was made by normalizing the amount of total protein from adult head loaded on the gel by BCA and then blotting for rhodopsin, in effect comparing the rations of eye tissue present in the same amount of total head tissue (Figure 3.5).

As expected, wild type samples showed robust levels of rhodopsin expression, indicating a plethora of functional photoreceptors present in the adult eye. *alg10* mutants expressed a reduced level of rhodopsin and *alg9* showed no sign of functional rhodopsin production. The *alg10* rescue shows levels of rhodopsin expression greater than both the *alg9* and *alg10* phenotypes, though still slightly less than the wild type adult (Figure 3.5).

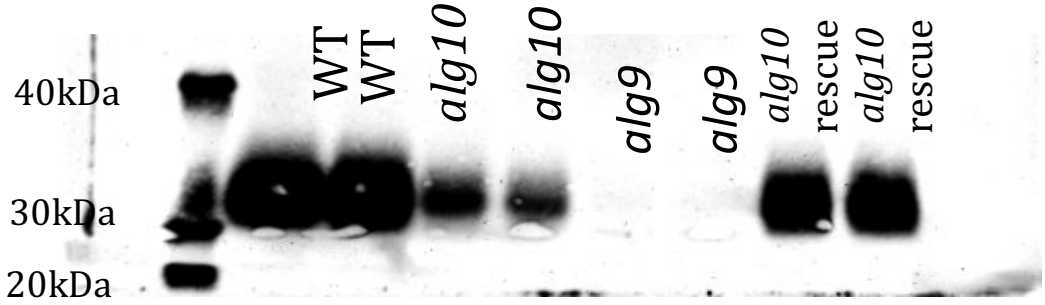

Figure 3.5 **:** Western blot of rhodopsin protein extracted from adult fly heads. *alg10* rescue shows expression levels significantly higher than *alg10* and comparable to wild type suggesting successful rescue of eye tissue.

Chapter 4

DISCUSSION

Congenital disorders of glycosylation are an under diagnosed and growing group of diseases that warrant further study in order to determine the molecular defects that cause their pleiotropic effects in humans. *Drosophila* offer the unique opportunity to study these diseases by targeting homozygous mutation to non-essential tissues allowing for study of the disease at all stages of development. Targeting mutation of *alg9* and a*lg10* has allowed us to study the effects of these mutations on developing neurons. This information is especially pertinent considering that most classes of CDG involve some level of nervous system abnormalities.

This research was focused first on gathering information about the overall organization of the eye disc in wild type, both mutants, and *alg10* rescue larva by immunofluorescence staining of the third instar imaginal eye disc. These experiments revealed a loss of the highly ordered compound eye structure found in the wild type eye in both mutant lines (Figure 3.1) . The *alg10* phenotype proved to be much less severe than the *alg9* phenotype. This difference likely arises from the fact that *alg10* is responsible for addition of the terminal glucose residue to the glycan one step prior to it's transfer to a target protein. *alg9,* acting twice and several steps earlier in the pathway, would be predicted to produce glycans more severely under developed than *alg10*. While the *alg10* mutant glycans may be transferred by the permissive B isoform of Ost, glycans synthesized in *alg9* mutant cells likely never make it to their target proteins. This total lack of glycosylation events could account for the extreme phenotype seen in the developing eye.

Also of note, is that the terminal glucose residue added by *alg10* is one of the three glucose residues trimmed from glycans before leaving the endoplasmic reticulum (Drickamer, 2006). These three glucose residues act as a quality control mechanism. They are removed as single glucose molecules, and removal of the third and final glucose residue signals that the glycoprotein is properly folded and ready for export to the Golgi for further modification (Drickamer 2006). The native transient nature of this third glucose residue could also account for the reduced severity of this phenotype. Since it is not naturally present outside of the ER, glycoproteins that do make it to their final destinations are likely fully functional. The *alg10* rescue showed a phenotype intermediate of the *alg10* and wild type (figures 3.1, 3.2, 3.6, and 3.7). This indicates that re-expression of *alg10* can repair the effects of its knockdown. It was also at this point that the absences of some photoreceptors in each of the oldest ommatidial clusters was noted, which will soon be discussed further.

Several glycoproteins were also studied using immunofluorescence staining. The most successful of these, chaoptin and neuroglian, revealed significant amounts of protein in non-native target areas, mainly the body of photoreceptor cells (figures 3.1, 3.2, and 3.3). This improper localization indicates two possible events: improper trafficking of glycoproteins to their target sites and retention of protein within the ER. As stated earlier, the trimming of three terminal glucose residues from a mature glycan is a mechanism by which the ER recognizes properly folded glycoproteins and prepares them from export to the Golgi (Drickamer 2006). *alg9* mutants that lack residues upstream of these glucose residues encounter two problems. The first is that Ost, though it has two isoforms, one allowing transfer of incomplete glycans and one only transferring properly formed glycans, is not known to transfer glycans lacking

several mannose residues (Ruiz 2011). This means that most (if not all) of the proteins intended to receive glycans do not in *alg9* mutants. Those proteins that do receive glycans are incapable of recognition by the quality control mechanism and may also compromise intracellular targeting. It is likely that due to this mechanism, most glycoproteins in *alg9* mutants are retained within the ER, as they lack a mechanism to recognize their proper folding which allows them to move on to the next step in development. Co-localization studies of glycoproteins and the ER could be useful in determining whether retention of glycoprotein in the cell bodies is due to improper trafficking or to retention of improperly folded protein in the ER.

Other antibodies for glycoprotein targets were tested against the eye tissue with varying degrees of success. Rhodopsin, used in other experiments on adult tissue, proved to be expressed later in development than expected, yielding no staining in the third instar disc. Members of the fascilin family and cadherin proved difficult to visualize consistently and showed no interesting phenotype. Additional studies of these proteins would be necessary to exclude them from use in this panel.

Noting the results of these initial studies, the focus of this project shifted to apoptosis and the possible mechanisms of its induction in the aging photoreceptor cell. Stainings with cleaved caspase 3 revealed that neuronal cells perceived to be missing through ELAV staining expressed high levels of this pro-apoptotic protein, a phenotype not seen in the wild type (figures 3.6 and 3.7) . Due to the build up of protein seen in the cell bodies and the late onset of apoptosis, induction of the unfolded protein response was considered the most likely mode of apoptotic induction. The UPR's first action is to trigger pro-survival pathways in an attempt to correct an overload of unfolded or misfolded protein in the ER, but exposure to prolonged stress

causes it to switch to pro-apoptotic functions (Tabas 2011). This mechanism matched the observed phenomena well, and the induction of UPR has been observed in other points in the N-linked pathway (Shaik 2011).

Several methods to study this pathway have been considered. IRE1 phosphorylates JNK as the initial step in its pro-apoptotic cascade, but unfortunately availability of JNK antibody has prevented western blot comparison of the levels of JNK phosphorylation (Tabas 2011). Flies expressing XBP1-GFP construct in the developing eye have been obtained from Ryoo *et al*. (2007). Successful generation of a balanced stock expressing both the XBP-GFP construct and the *alg9* or *alg10* mutations has been executed, and a positive control experiment is currently being optimized to confirm the activity of XBP1-GFP. Following the stress induction methods of Ryoo *et al.* (2007) has proved difficult as tissues subject to their protocol degraded to the point of uselessness. The protocol has now been optimized for future use. Also of interest is the transcription factor eIF2α. This transcription factor is part of the PERK mediated arm of the UPR (Figure 1.2). Upon stress induction PERK phosphorylates eIF2α, inhibiting its translational activity and decreasing global protein synthesis (Ron 2007). Examining levels of phosphorylated eIF2α could prove to be another door into understanding the induction of UPR. Being a complex, three-pronged pathway, there are many points at which UPR induction could be studied. Finding one with the proper reagents and usability in the *Drosophila* model is a challenging and an ongoing quest.

Further work in this and other areas could expand this project in different directions. Initial western blotting of target glycoproteins revealed no significant results; however, samples were taken from adult eyes, which are finished developing

and have already undergone mass apoptosis. It is possible that study of these proteins at the third instar larval stage may yield different results. As noted earlier, co-localization studies may be of interest to determine at which step proper trafficking of glycoproteins is being interrupted. Staining for markers specific to photoreceptors R1-R8 may also reveal a pattern to the cell death seen in the mutant phenotypes.

As the project stands with the results presented in this thesis, the following conclusions can be drawn:

1. *alg9* and *alg10* photoreceptor cells successfully acquire neuronal identity.

2. Both mutants show loss of typical ommatidial organization with *alg9* exhibiting a far more severe phenotype.

3. Aging photoreceptors in both mutant lines exhibit apoptosis leading to decreased levels of functional photoreceptors in the adult eye.

4. Both mutants show retention of target glycoprotein in the cell bodies, which could be due to the retention of protein within the ER or to improper trafficking through the secretory pathway.

5. Axons of both *alg9* and *alg10* mutant photoreceptors show loss of gathering at the optic nerve, which could be due to loss of function in cell-cell adhesion molecules and may also be the result of improper axon pathfinding.

REFERENCES

Bieber, A. J., Snow, P. M., Hortsch, M., Patel, N. H., Jacobs, J. R., Traquina, Z. R., ... & Goodman, C. S. (1989). Drosophila neuroglian: a member of the immunoglobulin superfamily with extensive homology to the vertebrate neural adhesion molecule L1. *Cell*, *59*(3), 447-460.

Beumer, K. J., Pimpinelli, S., & Golic, K. G. (1998). Induced chromosomal exchange directs the segregation of recombinant chromatids in mitosis of Drosophila. *Genetics*, *150*(1), 173-188.

Brand, A. H., & Perrimon, N. (1993). Targeted gene expression as a means of altering cell fates and generating dominant phenotypes.*development*, *118*(2), 401-415.

Burda, P., & Aebi, M. (1999). The dolichol pathway of N-linked glycosylation. *Biochimica et Biophysica Acta (BBA)-General Subjects*, *1426*(2), 239-257.

Calfon, M., Zeng, H., Urano, F., Till, J. H., Hubbard, S. R., Harding, H. P., ... & Ron, D. (2002). IRE1 couples endoplasmic reticulum load to secretory capacity by processing the XBP-1 mRNA. *Nature*, *415*(6867), 92-96.

Cruz, Y. P. 1993. "Laboratory Exercise in Developmental Biology." Academic Press: San Diego, California. pp. 214-228.

Drickamer K, Taylor ME (2006). Introduction to Glycobiology (2nd ed.). Oxford University Press, USA. ISBN 978-0-19-928278-4.

Freeman, M. (1997). Cell determination strategies in the Drosophila eye. *Development*, *124*(2), 261-270.

Jaeken, Jaak. Congenital Disorders of Glycosylation - NORD (National Organization for Rare Disorders). (2015). Retrieved May 09, 2016, from http://rarediseases.org/rare-diseases/congenital-disorders-of-glycosylation/

Jaeken, Jaak, and Lambert van den Heuvel. "Congenital disorders of glycosylation." *Physician's Guide to the Diagnosis, Treatment, and Follow-Up of Inherited Metabolic Diseases*. Springer Berlin Heidelberg, 2014. 483-512.

Hartwell, L., Hood, L., Goldberg, M., Reynolds, A., Silver, L., & Veres, R. (2006). Genetics: from genes to genomes. McGraw-Hill.

Hennet, Thierry. (2012). Diseases of glycosylation beyond classical congenital disorders of glycosylation. Biochimica et Biophysica Acta, (1820), 1306-1317.

Katanosaka, K., Tokunaga, F., Kawamura, S., & Ozaki, K. (1998). N-linked glycosylation of Drosophila rhodopsin occurs exclusively in the amino-terminal domain and functions in rhodopsin maturation. *FEBS letters*, *424*(3), 149-154.

Oslowski, C. M., & Urano, F. (2011). Measuring ER stress and the unfolded protein response using mammalian tissue culture system. *Methods in enzymology*, *490*, 71.

Purves, D. C., & Brachmann, C. (2007). Dissection of imaginal discs from 3rd instar Drosophila larvae.*Journal of visualized experiments: JoVE*, (2).

Robinow, S., & White, K. (1991). Characterization and spatial distribution of the ELAV protein during Drosophila melanogaster development. *Journal of neurobiology*, *22*(5), 443-461.

Ron, D., & Walter, P. (2007). Signal integration in the endoplasmic reticulum unfolded protein response. *Nature reviews Molecular cell biology*,*8*(7), 519-529.

Ruiz-Canada, C., Kelleher, D. J., & Gilmore, R. (2009). Cotranslational and posttranslational N-glycosylation of polypeptides by distinct mammalian OST isoforms. *Cell*, *136*(2), 272-283.

Ryoo, H. D., Domingos, P. M., Kang, M. J., & Steller, H. (2007). Unfolded protein response in a Drosophila model for retinal degeneration. *The EMBO journal*, *26*(1), 242-252.

Shaik, K. S., Pabst, M., Schwarz, H., Altmann, F., & Moussian, B. (2011). The Alg5 ortholog wollknäuel is essential for correct epidermal differentiation during drosophila late embryogenesis. Glycobiology, 21(6), 743-756.

Song, Z., Guan, B., Bergman, A., Nicholson, D. W., Thornberry, N. A., Peterson, E. P., & Steller, H. (2000). Biochemical and Genetic Interactions betweenDrosophila Caspases and the Proapoptotic Genesrpr, hid, and grim. *Molecular and cellular biology*, *20*(8), 2907-2914.

St. Johnston, D. (2002). The art and design of genetic screens: Drosophila melanogaster. Nature Reviews Genetics, 3, 176-188. doi: 10.1038/nrg751

Tabas, I., & Ron, D. (2011). Integrating the mechanisms of apoptosis induced by endoplasmic reticulum stress. *Nature cell biology*, *13*(3), 184-190.

Van Vactor, D., Krantz, D. E., Reinke, R., & Zipursky, S. L. (1988). Analysis of mutants in chaoptin, a photoreceptor cell-specific glycoprotein in Drosophila, reveals its role in cellular morphogenesis. *Cell*, *52*(2), 281-290.

Appendix A

GENETIC CROSSES

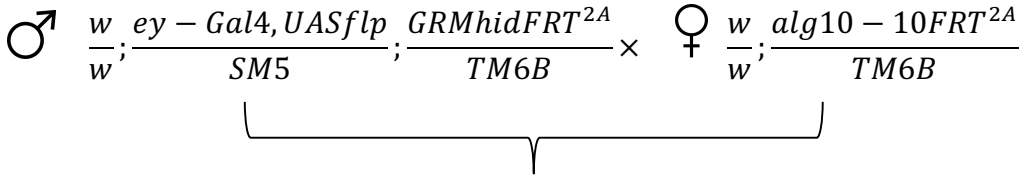

Collect third instar larva lacking Tb phenotype, homologous recombination occurs in the eye tissue only, resulting in homozygous mutant eye tissue. Collect adults with rough eye and non-stubble phenotype.

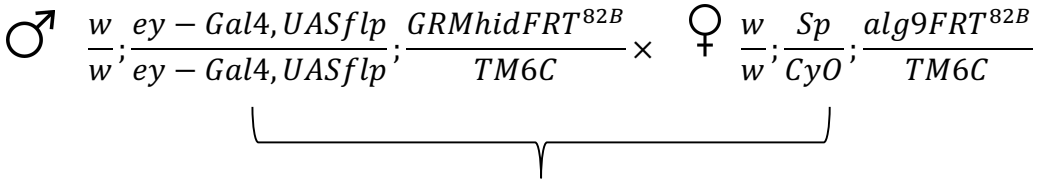

Collect third instar larva lacking Tb phenotype, homologous recombination occurs in the eye tissue only, resulting in homozygous mutant eye tissue. Collect adults with rough eye and non-stubble phenotype.

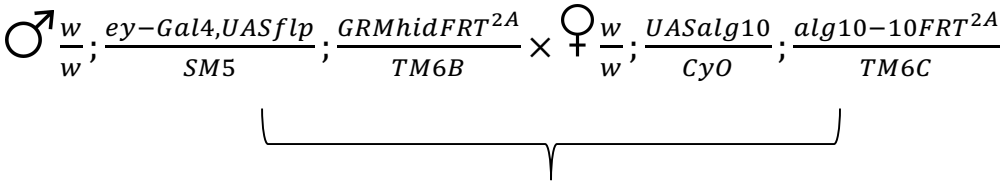

Collect third instar larva lacking Tb phenotype, homologous recombination occurs in the eye tissue only, resulting in homozygous mutant eye tissue. Collect adults with rough eye and non-stubble phenotype.

Appendix B

ANTIBODIES

Primary antibody	Abbreviation	Dilution	source
Rat α ELAV	RtαELAV	1:100	DSHB[1]
Mouse α ELAV	MαELAV	1:100	DSHB[1]
Mouse α neuroglian	MαBP102	1:100	DSHB[1]
Mouse α wingless	MαWg	1:10	DSHB[1]
Rabbit α caspase 3	RbαCaspase	1:100	Cell Signalling
Mouse α chaoptin	Mα24B10	1:100	DSHB[1]
Mouse α Fascilin I	MαFasI	1:100	DSHB[1]
Mouse α Fascilin II	MαFasII	1:100	DSHB[1]
Mouse α Fascilin III	MαFasIII	1:100	DSHB[1]
Rat α Cadherin	MαECad	1:100	DSHB[1]
Mouse α Rhodopsin	MαRh	1:100	DSHB[1] (western)

1. Developmental Studies Hybridoma Bank

Secondary antibody	Abbreviation	Dilution	source
Goat α mouse 488	GαM488	1:500	Invitrogen
Goat α mouse 568	GαM568	1:500	Invitrogen
Goat α Rat 488	GαRt488	1:500	Invitrogen
Goat α rabbit 488	GαRb488	1:500	Invitrogen
Goat α mouse HRP	GαHRP	1:5000	Jackson laboratory